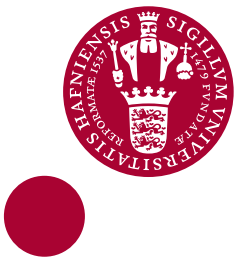

Unusually large Stokes shift for a near-infrared emitting DNA-stabilized silver nanocluster

Bogh, Sidsel Ammitzbøll; Carro-Temboury, Miguel R.; Cerretani, Cecilia; Swasey, Steven M.; Copp, Stacy M.; Gwinn, Elisabeth G.; Vosch, Tom

Published in:
Methods and Applications in Fluorescence

DOI:
10.1088/2050-6120/aaa8bc

Publication date:
2018

Document version
Publisher's PDF, also known as Version of record

Methods and Applications in Fluorescence

PAPER • OPEN ACCESS

Unusually large Stokes shift for a near-infrared emitting DNA-stabilized silver nanocluster

Methods and Applications in Fluorescence

PAPER

Unusually large Stokes shift for a near-infrared emitting DNA-stabilized silver nanocluster

Sidsel Ammitzbøll Bogh[1], Miguel R Carro-Temboury[1], Cecilia Cerretani[1], Steven M Swasey[2], Stacy M Copp[3,4], Elisabeth G Gwinn[3] and Tom Vosch[1]

[1] Nanoscience Center & Department of Chemistry, University of Copenhagen, Universitetsparken 5, DK-2100 Copenhagen, Denmark
[2] Chemistry Department UCSB, Santa Barbara California 93117, United States of America
[3] Physics Department UCSB, Santa Barbara California 93117, United States of America
[4] Current address: Center for Integrated Nanotechnologies, Los Alamos National Laboratories, Los Alamos, NM 87545, United States of America

E-mail: tom@chem.ku.dk

OPEN ACCESS

RECEIVED
3 November 2017

REVISED
9 December 2017

ACCEPTED FOR PUBLICATION
18 January 2018

PUBLISHED
9 February 2018

Keywords: silver nanocluster, fluorescence, excited state relaxation, time-resolved emission spectra, near-IR emitter, time-correlated single photon counting

Supplementary material for this article is available online

Abstract

In this paper we present a new near-IR emitting silver nanocluster (NIR-DNA-AgNC) with an unusually large Stokes shift between absorption and emission maximum (211 nm or 5600 cm^{-1}). We studied the effect of viscosity and temperature on the steady state and time-resolved emission. The time-resolved results on NIR-DNA-AgNC show that the relaxation dynamics slow down significantly with increasing viscosity of the solvent. In high viscosity solution, the spectral relaxation stretches well into the nanosecond scale. As a result of this slow spectral relaxation in high viscosity solutions, a multi-exponential fluorescence decay time behavior is observed, in contrast to the more mono-exponential decay in low viscosity solution.

1. Introduction

Due to its sensitivity and versatility, fluorescence spectroscopy has found many applications in both materials and life science imaging [1, 2]. As a result, a myriad of different emitters have been developed over the years [1]. Among these, DNA-stabilized silver nanoclusters (DNA-AgNCs) are a new class of emitters that were introduced in 2004 [3]. DNA-AgNCs exhibit a wide range of emission properties that can be tuned by changing the stabilizing DNA sequence [4–8]. The DNA-AgNCs usually contain below 25 silver atoms [9] and in some cases form bright and photo-stable emitters, though dark clusters are often formed as well [10–12]. Despite numerous applications in sensing [13–18], relating the photophysical properties to compositional and structural properties is still an active and ongoing research topic [17, 19–24]. For most fluorescence imaging applications, bright emitters with high photo-stability and a reasonable Stokes shift are used to create contrast. The Stokes shift in particular is useful for spectrally separating the excitation light from the probe emission [25].

The DNA-AgNC that we introduce here has an unusually large Stokes shift, which to the best of our knowledge is the largest reported Stokes shift (211 nm or 5600 cm^{-1}) for any DNA-AgNC. For comparison, a recent review on fluorescent dyes with large Stokes shift did not present any fluorophores with a Stokes shift above 160 nm in the emission region above 600 nm [26]. Besides the large Stokes shift, another remarkable property is the emission of the DNA-AgNC in the near-infrared (NIR) part of the electromagnetic spectrum, a region that is of particular interest for tissue imaging since biological material and tissue have a window of high transparency in the 650–900 nm range [27]. The use of DNA-AgNCs in bioimaging has already been demonstrated in several studies [28–32].

The particular DNA sequence that stabilizes this DNA-AgNC, 5′-CACCTAGCGA-3′, was discovered as part of a larger study of the relation between silver cluster color and the properties of the host DNA strand [33]. The photophysical characterization of the NIR emitting DNA-AgNC (NIR-DNA-AgNC) presented here provides insight into the temporal and

spectral relaxation of the excited state, which could facilitate the future use of NIR-DNA-AgNC and other DNA-AgNC emitters in a multitude of applications.

2. Materials and methods

2.1. Sample preparation

The NIR-DNA-AgNC was synthesized by mixing hydrated DNA (5′-CACCTAGCGA-3′, IDT DNA Technologies) with $AgNO_3$ (⩾99.998%, Sigma Aldrich) in a 10 mM ammonium acetate (NH_4OAc) buffer (pH 7.0) prepared in nuclease free water (IDT DNA Technologies). 15 min after mixing DNA and $AgNO_3$, the sample was reduced by 0.5 equivalents $NaBH_4$ (99.99%, Sigma Aldrich) per silver cation. The final ratio of [DNA]:[Ag^+]:[BH_4^-] was [1]:[7.5]:[3.75], and the concentration of DNA in the synthesis was found to be optimal at 25 μM. The sample was kept in the fridge for three days prior to HPLC purification. After purification, the solvent was exchanged to 10 mM NH_4OAc since DNA-AgNCs have a high stability in this buffer. The remarkable stability of NIR-DNA-AgNC in 10 mM NH_4OAc is illustrated in figure S5 is available online at stacks.iop.org/MAF/6/024004/mmedia, which shows negligible change in absorbance for the NIR-DNA-AgNC two months after purification.

2.2. HPLC purification

The HPLC purification was performed using a preparative HPLC system from Agilent Technologies with an Agilent Technologies 1260 infinity fluorescence detector and a Kinetex C18 column (5 μm, 100 Å, 50 × 4.6 mm). The mobile phase was a gradient mixture of methanol and water with 35 mM triethylammonium acetate (TEAA). The gradient was varied from 15% to 95% TEAA in methanol in 24 min. In the time range 2–22 min the gradient flow was increased linearly from 20% to 40% TEAA in methanol. The fraction collected at ~35% TEAA in MeOH (17 min elution time) contained the NIR-DNA-AgNC, which was identified using the absorbance signal at 530 nm. The flow rate was 1.3 ml min^{-1}. The run was followed by 6 min of washing with 95% TEAA in methanol to remove any remaining sample from the column.

2.3. Steady-state absorption and emission spectroscopy

All absorption measurements were carried out on a Lambda 1050 instrument from Perkin Elmer using a deuterium lamp for ultraviolet radiation and a halogen lamp for visible and near infrared radiation. Steady-state fluorescence measurements were done using either a Fluotime 300 instrument from PicoQuant with a 532 nm laser as excitation source, or using a QuantaMaster 400 from PTI with a xenon arc lamp as excitation source. For all fluorescence measurements the absorption was kept below 0.1 to avoid inner filter effects. All fluorescence spectra were corrected for the wavelength dependency of the detector system.

2.4. Time-correlated single photon counting

TCSPC measurements were conducted using a Fluotime 300 instrument from PicoQuant with a 532 nm pulsed laser (PicoQuant) as excitation source for all experiments. The data was analyzed using Fluofit v.4.6 software from PicoQuant.

3. Results and discussion

3.1. Steady-state results

The stabilizing single stranded DNA scaffold used in this study consists of the 10 base sequence 5′-CACCTAGCGA-3′ [33]. The formation kinetics of the NIR-DNA-AgNC is slow: to obtain a good synthesis yield, it is best to perform the HPLC purification at least three days after synthesis (see figure S1). Figure S2 shows the HPLC traces of the synthesized NIR-DNA-AgNC sample. The NIR-DNA-AgNC studied in this paper was collected in the fraction that eluted around 17 min after injection. As depicted in figure 1(A), the NIR-DNA-AgNC in a solution of 10 mM NH_4OAc has an absorption maximum in the visible region at 525 nm and an emission maximum at 736 nm at 25 °C. Even though this is a significantly large Stokes shift (211 nm or 5600 cm^{-1}) and the emission spectrum is very broad when plotted as a function of wavelength, the plot of 2D excitation versus emission in figure 1(B) shows only a single feature. Excitation spectra measured at different emission wavelengths (650–800 nm) all give nearly identical spectra, similar to the shape of the absorption spectrum, which implies that only one emissive species is present (figure S3) [1]. By plotting the absorption and emission spectra on a wavenumber scale (figure S4), it is clear that the widths of the absorbance and the emission peaks are similar (the broad emission spectrum on a wavelength scale is due to the smaller energy step size between each nm at higher wavelengths; see figures 1(A) and S4). One note of caution is that the tail of the emission is approaching the sensitivity edge of the detector so, despite careful correction for the variation in the detector sensitivity at this wavelength range, some error on the determined intensity could be present (see SI). The large Stokes shift and emission ranging from 600 nm to more than 850 nm make determination of the fluorescence quantum yield challenging. Nevertheless, we calculate a quantum yield value of 0.26 using Cresyl Violet in absolute ethanol as a reference (see SI for more details).

In a previous study, we investigated a red emitting DNA-AgNC (red-DNA-AgNC) that exhibits a red-shift in the emission maximum as temperature is increased. This temperature-dependent spectral shift of red-DNA-AgNC was attributed to a faster relaxation to an energetically more relaxed excited state, at

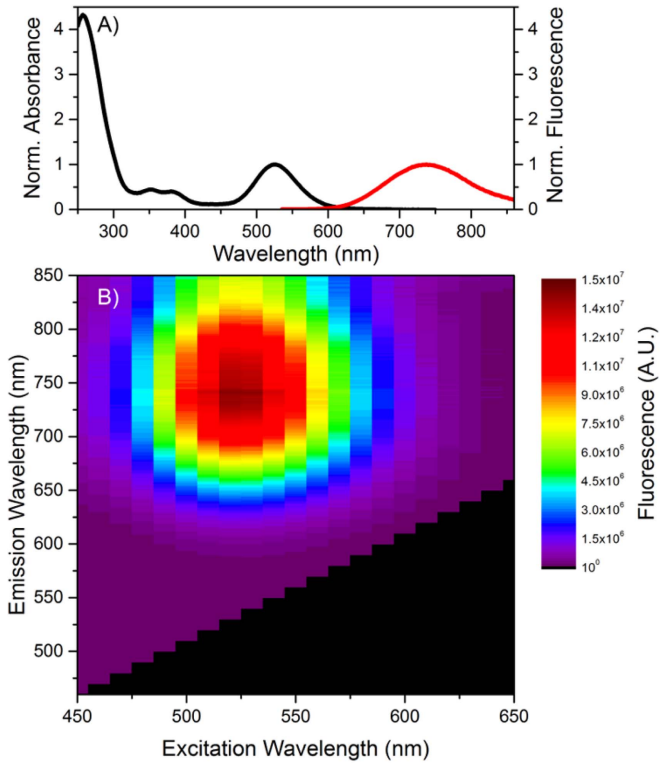

Figure 1. NIR-DNA-AgNC in 10 mM NH_4OAc at room temperature. (A) Normalized absorption (black line) and normalized emission (red line) spectra exciting at 532 nm. (B) Steady-state 2D excitation versus emission plot.

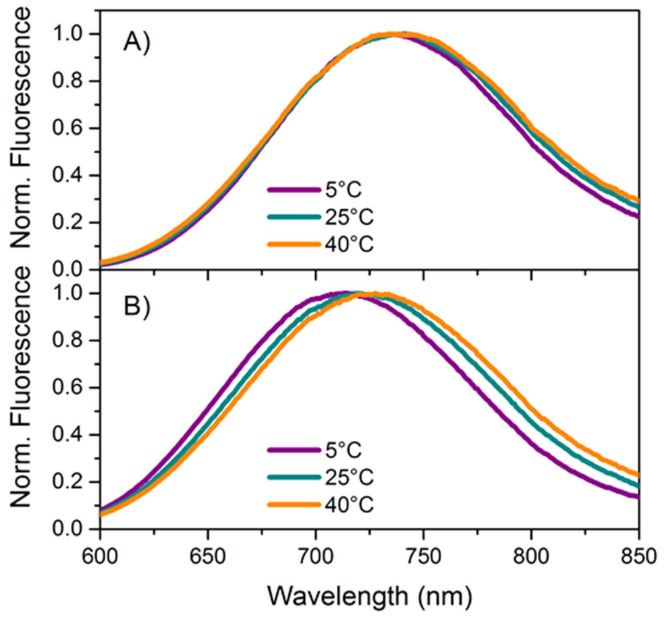

Figure 2. (A) Normalized emission spectra at different temperatures for NIR-DNA-AgNC in 10 mM NH4OAc. (B) Normalized emission spectra at different temperatures for NIR-DNA-AgNC in 90% glycerol and 10% 10 mM NH_4OAc. All spectra have been normalized to highlight the shift of the emission maximum. It should be noted that the fluorescence intensity does change with temperature as well.

higher temperature [34]. However, it was unclear whether the increased thermal energy, decreased viscosity, or a combination of both caused this effect. Here, we performed temperature dependent fluorescence measurements for the NIR-DNA-AgNC to investigate if a spectral shift is present. The emission spectra in figure 2(A) reveal minor spectral shifts of the NIR-DNA-AgNC in 10 mM NH_4OAc as a function of temperature at 5, 25 and 40 °C. If temperature controls the magnitude of energy relaxation after

Table 1. Absorption λ_{abs}(max) and emission λ_{em}(max) maxima, fluorescence quantum yield QY, weighted average fluorescence decay time $\langle\tau_w\rangle$ and average fluorescence lifetime $\langle\tau\rangle$ (excitation at 532 nm), for NIR-DNA-AgNC at different temperatures and in low (10 mM NH_4OAc) and high viscosity (90% glycerol, 10% 10 mM NH_4OAc) solutions.

	T (°C)	λ_{abs}(max)	λ_{em}(max)	QY[a]	$\langle\tau_w\rangle$[b]	$\langle\tau\rangle$[c]
Low viscosity	5	525 nm	735 nm			3.70 ns
	25	525 nm	736 nm	0.26	3.27 ns	3.26 ns
	40	524 nm	737 nm			2.99 ns
High viscosity	5	521 nm	715 nm			3.99 ns
	25	522 nm	720 nm	0.27	3.58 ns	3.69 ns
	40	524 nm	728 nm			3.50 ns

[a] The fluorescence quantum yield was measured using Cresyl Violet in absolute ethanol (QY = 0.56) as reference compound [37].

[b] Average decay time, weighted by the intensity over the whole emission range.

[c] Average decay time of NIR-DNA-AgNC at 730 nm detection for 10% 10 mM NH_4OAc and 720 nm for 90% glycerol, 10% 10 mM NH_4OAc.

excitation, as hypothesized for the previously studied red-DNA-AgNC, one might expect that due to the large Stokes shift of NIR-DNA-AgNC in 10 mM NH_4OAc, NIR-DNA-AgNC would show even larger temperature dependent shift. However, the minor temperature-dependent spectral shift of NIR-DNA-AgNC leads us to speculate that the spectral relaxation could be much faster for NIR-DNA-AgNC than the relaxation we measured for red-DNA-AgNC. If the relaxation time is much faster than the excited state decay time, we suspected that increasing the viscosity could change the rate of the spectral relaxation for NIR-DNA-AgNC. To test this hypothesis, we increased the viscosity in an attempt to slow down the excited state spectral relaxation, studying the steady-state emission properties of NIR-DNA-AgNC in a mixture of 90% glycerol (volume percent) and 10% 10 mM NH_4OAc in water. Changing the viscosity by addition of glycerol will also change other solvent properties, e.g. polarity, which also play a role in the differences in the absorption and emission maxima [35, 36] (see table 1), but here we keep the amount of glycerol in the high viscosity solution constant and only look at the effect of temperature on the emission spectra. The effect of changing the dielectric constant of the solvent was investigated previously by Copp *et al* and it was shown that dielectric-dependent spectral changes did not follow a Lippert–Mataga based model. Specific solvent interaction with the DNA scaffold might play a more important role on the spectral shift [36]. As shown in figure 2(B), we observe a clear temperature-dependent spectral shift.

The large shift between absorption and emission maxima points to a significant relaxation between the initial Frank Condon state and the emission from the S_1 state of the fluorophore [34]. This spectral relaxation seems to happen (figure 2(A)) on a time-scale that is faster than the S_1 decay time in 10 mM NH_4OAc, resulting in a minimal temperature dependent shift in the emission maximum. Increasing the viscosity of the solvent seems to slow down this spectral relaxation process (figure 2(B)), resulting in a shift of emission maximum with temperature. To investigate the hypothesis that viscosity determines the extent and temperature dependence of the spectral relaxation, we performed time-resolved fluorescence measurements on the NIR-DNA-AgNC in both the low and high viscosity solutions.

3.2. Time-resolved results

Previously we have shown that for red-DNA-AgNCs, a spectral relaxation that extends into the nanosecond time scale is present [34]. This results in an apparent multi-exponential decay behavior and complicated decay associated spectra. However, analyzing the data by creating time-resolved emission spectra (TRES) is a more convenient and clearer way to represent the temporal and spectral relaxation of the excited state. Figure 3 shows the results of NIR-DNA-AgNC in low viscosity (10 mM NH_4OAc) and high viscosity (90% glycerol, 10% 10 mM NH_4OAc) solutions at 25 °C.

The TRES in figure 3(A) and average decay time spectrum in figure 3(B) show that only a minimal spectral shift is present for varying time points for NIR-DNA-AgNC in low viscosity solution. This indicates that most of the spectral relaxation for the low viscosity case must take place on a time scale below the IRF resolution of the equipment used here (~150 ps). From our steady state hypothesis, we expected that as viscosity increases, the spectral relaxation would slow down. Figures 3(C) and (D) show the TRES and average decay time spectrum in high viscosity solution. The average fluorescence decay time spectrum concurrently rises from around 2.7 ns at 600 nm emission to 4.2 ns at 860 nm emission, which one would expect for a slow spectral relaxation on the time scale of the excited state decay time [1]. Now that we have been able to show that our viscosity hypothesis holds (that the viscosity of the solvent can kinetically hinder the excited state to reach its fully relaxed state) and is verified by the time-resolved results, one intriguing question remains: what is the mechanism causing the

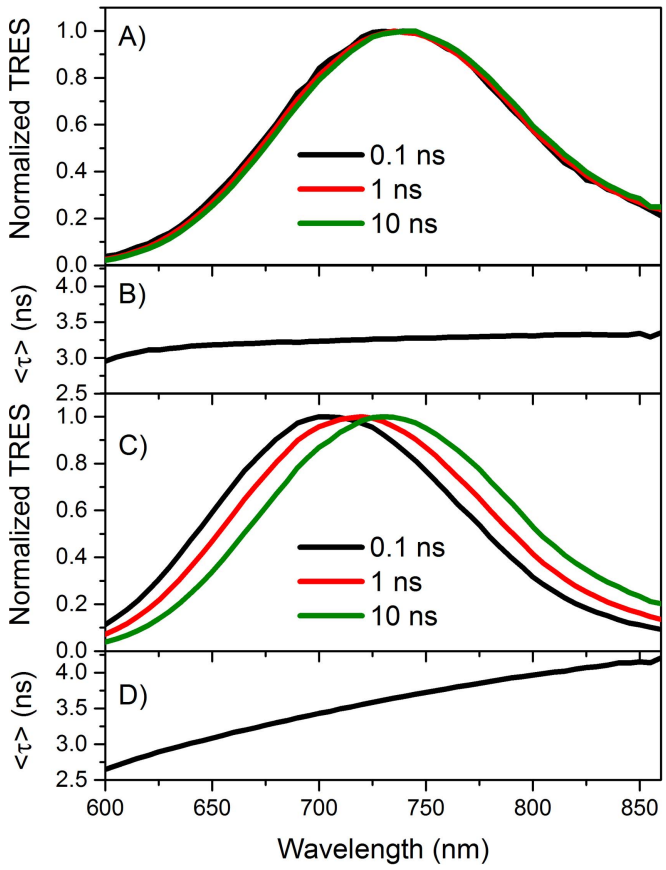

Figure 3. (A) Time-resolved emission spectra of NIR-DNA-AgNCs at 25 °C in 10 mM NH_4OAc. (B) Average fluorescence decay time as a function of emission wavelength in 10 mM NH_4OAc. (C) Time-resolved emission spectra of NIR-DNA-AgNCs at 25 °C in 90% glycerol, 10% 10 mM NH_4OAc. (D) Average fluorescence decay time as a function of emission wavelength in 90% glycerol, 10% 10 mM NH_4OAc.

different spectral relaxation speed for NIR-DNA-AgNC and red-DNA-AgNC? The previously studied red-DNA-AgNC, which has much slower spectral relaxation in the low viscosity case, is stabilized by a much longer DNA oligomer (19 bases; 5′-TTCCCACCCACCCCGGCCC-3′) than the NIR-DNA-AgNC studied here, which is stabilized by an oligomer of 10 bases. Earlier studies suggest that it is unlikely that a near-IR emitting silver clusters would be stabilized by one single DNA strand of 10 bases [6], and studies of visibly emitting silver clusters stabilized by 10-base DNA strands have found that even for green and red silver clusters, two copies of a 10-base DNA strand are required [6, 16]. It is thus likely that the NIR-DNA-AgNC is stabilized by at least two DNA strands, and it could be that stabilization by two or more DNA strands instead of one longer DNA strand enables faster spectral relaxation. Such a hypothesis is only speculative at this point, and future studies correlating number of bases with spectral relaxation would be interesting. Additionally, it is also interesting to point out that the observed decay time behavior of purified NIR-DNA-AgNC can either be mono-exponential or multi-exponential, depending on the spectral relaxation speed [10]. This is demonstrated in table S1 and commented on more below. To get an idea about the hydrodynamic volume of NIR-DNA-AgNC in 10 mM NH_4OAc, we performed time-resolved anisotropy measurements (see figure S8). Tail-fitting the data with a single exponential rotational correlation time, we obtain a hydrodynamic volume of ~10.5 nm^3 for NIR-DNA-AgNC [1].

Finally, we investigated the effect of temperature on the average decay time for NIR-DNA-AgNC in low and high viscosity solutions. Figure S9 shows that the temperature can reversibly cycle between 5, 25 and 40 °C, with no impact on the stability of the NIR-DNA-AgNC. It is also seen that the NIR-DNA-AgNC emission intensity is temperature-dependent as was also observed for red-DNA-AgNC and other DNA-AgNCs [34, 38]. Examining the fluorescence decay curves for NIR-DNA-AgNC in figures 4(A) and (B) we observe a decreasing trend of average decay time, $\langle\tau\rangle$, with increasing temperatures. These results are in line with the previous red-DNA-AgNC results, where we showed that the decay time is temperature-dependent and can be used as a thermometer [34].

In figure 4(C), where three $\langle\tau\rangle$ values of NIR-DNA-AgNC are plotted as a function of temperature, we see linear trends in both 10 mM NH_4OAc (dots) and 90% glycerol, 10% 10 mM NH_4OAc (squares). The changes in $\langle\tau\rangle$ with temperature are similar in

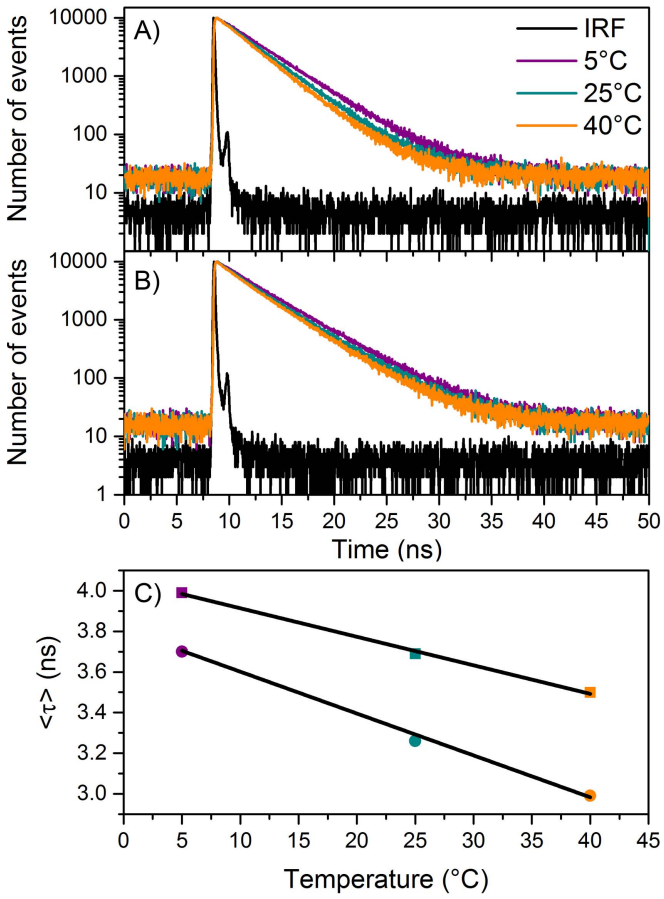

Figure 4. (A) Fluorescence decay curves for NIR-DNA-AgNC at different temperatures in 10 mM NH_4OAc. (B) Fluorescence decay curves for NIR-DNA-AgNC at different temperatures in 90% glycerol, 10% 10 mM NH_4OAc. (C) Average fluorescence decay times as a function of temperature in 10 mM NH_4OAc (dots) or in 90% glycerol, 10% 10 mM NH_4OAc (squares). The fluorescence decays were measured at emission wavelengths of 720 nm and 730 nm for 90% glycerol, 10% 10 mM NH_4OAc and 10 mM NH_4OAc, respectively, and the excitation wavelength was 532 nm in both cases.

high and low viscosity solutions (though the values of $\langle\tau\rangle$ vary), indicating that the change in decay time is mainly due to the temperature and not to temperature-induced changes in viscosity (see SI for further details). To illustrate this, we plotted the approximated viscosities of the solutions at different temperatures versus the emission maxima (in wavenumber scale). This data (figure S10) shows a monotonic dependence on these six data points we measured here. Further follow-up studies with more viscosity data points would be interesting to investigate this dependence in more detail.

As discussed previously, the multi-exponential character of the decay curves is greatly influenced by the speed of the spectral relaxation process. In the case of low viscosity solution, the spectral relaxation is too fast to be clearly resolved in the TCSPC resolution of the equipment; thus, the decay curve ($\lambda_{exc} = 532$ nm, $\lambda_{em} = 730$ nm) can be satisfactorily fitted with a single exponential decay (see table S1). However, in order to fit the decay curve of the NIR-DNA-AgNC in high viscosity solution ($\lambda_{exc} = 532$ nm, $\lambda_{em} = 720$ nm), a single exponential model is clearly not satisfactory. Instead, a two or three exponential model is required to get a good fit due to the spectral shift of the emission maximum in the nanosecond time scale (table S1).

4. Conclusions

We present a new near-IR emitting DNA-AgNC with an unusually large Stokes shift (211 nm or 5600 cm^{-1}). The steady-state properties of NIR-DNA-AgNC show that there is only a minimal spectral shift with changing temperature in 10 mM NH_4OAc. However, in a solution with much higher viscosity, a clear temperature dependent spectral shift in the emission spectrum is apparent. The same trend is evident from time-resolved measurements of NIR-DNA-AgNC in high viscosity solution, where time-resolved spectral relaxation is now stretched to the nanosecond time scale. At low viscosity, most of the spectral relaxation happens on a time scale faster than our TCSPC equipment can resolve (~150 ps). Fast spectral relaxation makes time-resolved TCSPC data less complicated to analyze and could therefore be an advantage in potential sensing or imaging applications. It can also help explain why some purified DNA-AgNCs exhibit mono-exponential decay while others decay multi-

exponentially. We speculate that the length of the DNA sequence and/or flexibly could be a determining factor in the spectral relaxation speed. Future studies should address this question.

Acknowledgments

TV, SAB, MR C-T and CC gratefully acknowledge financial support from the 'Center for Synthetic Biology' at Copenhagen University funded by the UNIK research initiative of the Danish Ministry of Science, Technology and Innovation (Grant 09-065274), bioSYNergy, University of Copenhagen's Excellence Programme for Interdisciplinary Research, the Villum Foundation (Project number VKR023115), HFSP (RGY0081/2014) and the Carlsberg Foundation (CF14-0388). SMC, SMS and EGG acknowledge support from NSF grant DMR 1309410. We thank Sruthi Gudibandi and Petko Bogdanov for their contributions to development of the DNA sequence reported here. The authors declare no conflicts of interest.

ORCID iDs

Sidsel Ammitzbøll Bogh https://orcid.org/0000-0001-9827-6205
Miguel R Carro-Temboury https://orcid.org/0000-0003-2817-9172
Tom Vosch https://orcid.org/0000-0001-5435-2181

References

[1] Lakowicz J R 2006 *Principles of Fluorescence Spectroscopy* 3rd edn (Berlin: Springer)
[2] Kubitscheck U 2017 *Fluorescence Microscopy: From Principles to Biological Applications* (New York: Wiley-VCH Verlag GmbH & Co. KGaA)
[3] Petty J T, Zheng J, Hud N V and Dickson R M 2004 DNA-templated Ag nanocluster formation *J. Am. Chem. Soc.* **126** 5207–12
[4] Richards C I, Choi S, Hsiang J C, Antoku Y, Vosch T, Bongiorno A, Tzeng Y L and Dickson R M 2008 Oligonucleotide-stabilized Ag nanocluster fluorophores *J. Am. Chem. Soc.* **130** 5038–9
[5] Sharma J, Yeh H C, Yoo H, Werner J H and Martinez J S 2010 A complementary palette of fluorescent silver nanoclusters *Chem. Commun.* **46** 3280–2
[6] Schultz D and Gwinn E G 2012 Silver atom and strand numbers in fluorescent and dark Ag:DNAs *Chem. Commun.* **48** 5748–50
[7] Sengupta B, Ritchie C M, Buckman J G, Johnsen K R, Goodwin P M and Petty J T 2008 Base-directed formation of fluorescent silver clusters *J. Phys. Chem.* C **112** 18776–82
[8] Zhang L and Wang E 2014 Metal nanoclusters: New fluorescent probes for sensors and bioimaging *Nano Today* **9** 132–57
[9] Gwinn E, Schultz D, Copp S M and Swasey S 2015 DNA-protected silver clusters for nanophotonics *Nanomaterials* **5** 180–207
[10] Choi S, Dickson R M and Yu J 2012 Developing luminescent silver nanodots for biological applications *Chem. Soc. Rev.* **41** 1867–91
[11] Latorre A and Somoza A 2012 DNA-mediated silver nanoclusters: synthesis, properties and applications *Chem. Biochem.* **13** 951–8
[12] Gwinn E G, O'Neill P, Guerrero A J, Bouwmeester D and Fygenson D K 2008 Sequence-dependent fluorescence of DNA-hosted silver nanoclusters *Adv. Mater.* **20** 279–83
[13] Ge L, Sun X M, Hong Q and Li F 2017 Ratiometric catalyzed-assembly of nanocluster beacons: a nonenzymatic approach for amplified DNA detection *ACS Appl. Mater. Interfaces* **9** 32089–96
[14] Xie P S, Zhan Y J, Wu M, Guo L H, Lin Z Y, Qiu B, Chen G N and Cai Z W 2017 The detection of melamine base on a turn-on fluorescence of DNA-Ag nanoclusters *J. Lumin.* **186** 103–8
[15] Li C Y and Wei C Y 2017 DNA-templated silver nanocluster as a label-free fluorescent probe for the highly sensitive and selective detection of mercury ions *Sensors Actuators* B **242** 563–8
[16] Schultz D, Gardner K, Oemrawsingh S S R, Markešević N, Olsson K, Debord M, Bouwmeester D and Gwinn E 2013 Evidence for rod-shaped DNA-stabilized silver nanocluster emitters *Adv. Mater.* **25** 2797–803
[17] Copp S M, Schultz D, Swasey S, Pavlovich J, Debord M, Chiu A, Olsson K and Gwinn E 2014 Magic numbers in DNA-stabilized fluorescent silver clusters lead to magic colors *J. Phys. Chem. Lett.* **5** 959–63
[18] Hsu H-C, Lin Y-X and Chang C-W 2017 The optical properties of the silver clusters and their applications in the conformational studies of human telomeric DNA *Dyes Pigments* **146** 420–4
[19] Petty J T, Ganguly M, Rankine I J, Chevrier D M and Zhang P 2017 A DNA-encapsulated and fluorescent Ag106+ cluster with a distinct metal-like core *J. Phys. Chem.* C **121** 14936–45
[20] Petty J T, Fan C, Story S P, Sengupta B, Sartin M, Hsiang J-C, Perry J W and Dickson R M 2011 Optically enhanced, near-IR, silver cluster emission altered by single base changes in the DNA template *J. Phys. Chem.* B **115** 7996–8003
[21] Bogh S A, Cerretani C, Kacenauskaite L, Carro-Temboury M R and Vosch T 2017 Excited-state relaxation and förster resonance energy transfer in an organic fluorophore/silver nanocluster dyad *ACS Omega* **2** 4657–64
[22] Thyrhaug E, Bogh S A, Carro-Temboury M R, Madsen C S, Vosch T and Zigmantas D 2017 Ultrafast coherence transfer in DNA-templated silver nanoclusters *Nat. Commun.* **8** 15577
[23] Neidig M L, Sharma J, Yeh H-C, Martinez J S, Conradson S D and Shreve A P 2011 Ag K-Edge EXAFS analysis of DNA-templated fluorescent silver nanoclusters: insight into the structural origins of emission tuning by DNA sequence variations *J. Am. Chem. Soc.* **133** 11837–9
[24] Berdakin M, Taccone M, Julian K J, Pino G and Sánchez C G 2016 Disentangling the photophysics of DNA-stabilized silver nanocluster emitters *J. Phys. Chem.* C **120** 24409–16
[25] Stokes G G 1852 On the change of refrangibility of light *Phil. Trans. R. Soc.* **142** 463–562
[26] Maksim V S, Vladimir N B and Stefan W H 2015 Fluorescent dyes with large Stokes shifts for super-resolution optical microscopy of biological objects: a review *Methods Appl. Fluoresc.* **3** 042004
[27] Weissleder R 2001 A clearer vision for *in vivo* imaging *Nat. Biotechnol.* **19** 316–7
[28] Yu J, Choi S and Dickson R M 2009 Shuttle-based fluorogenic silver-cluster biolabels *Angew. Chem., Int. Ed.* **48** 318–20
[29] Antoku Y, Hotta J.-I., Mizuno H, Dickson R M, Hofkens J and Vosch T 2010 Transfection of living HeLa cells with fluorescent poly-cytosine encapsulated Ag nanoclusters *Photochem. Photobiol. Sci.* **9** 716–21
[30] Yu J, Choi S, Richards C I, Antoku Y and Dickson R M 2008 Live cell surface labeling with fluorescent Ag nanocluster conjugates *Photochem. Photobiol.* **84** 1435–9
[31] Li J L, Zhong X Q, Cheng F F, Zhang J R, Jiang L P and Zhu J J 2012 One-pot synthesis of aptamer-functionalized silver nanoclusters for cell-type-specific imaging *Anal. Chem.* **84** 4140–6

[32] Han G-M, Jia Z-Z, Zhu Y-J, Jiao J-J, Kong D-M and Feng X-Z 2016 Biostable L-DNA-templated aptamer-silver nanoclusters for cell-type-specific imaging at physiological temperature *Anal. Chem.* **88** 10800–4
[33] Copp S M, Gorovitz A, Swasey S M, Gudibandi S, Bogdanov P and Gwinn E G 2018 Color by data-driven design of genomic silver clusters in preparation
[34] Cerretani C, Carro-Temboury M R, Krause S, Bogh S A and Vosch T 2017 Temperature dependent excited state relaxation of a red emitting DNA-templated silver nanocluster *Chem. Commun.* **53** 12556–9
[35] Copp S M, Schultz D, Swasey S M, Faris A and Gwinn E G 2016 Cluster plasmonics: dielectric and shape effects on DNA-stabilized silver clusters *Nano Lett.* **16** 3594–9
[36] Copp S M, Faris A, Swasey S M and Gwinn E G 2016 Heterogeneous solvatochromism of fluorescent DNA-stabilized silver clusters precludes use of simple onsager-based stokes shift models *J. Phys. Chem. Lett.* **7** 698–703
[37] Sens R and Drexhage K H 1981 Fluorescence quantum yield of oxazine and carbazine laser dyes *J. Lumin.* **24** 709–12
[38] Schultz D, Copp S M, Markešević N, Gardner K, Oemrawsingh S S R, Bouwmeester D and Gwinn E 2013 Dual-color nanoscale assemblies of structurally stable, few-atom silver clusters, as reported by fluorescence resonance energy transfer *ACS Nano* **7** 9798–807